Heliyon 9 (2023) e21010

Contents lists available at ScienceDirect

Heliyon

journal homepage: www.cell.com/heliyon

BMSCs alleviate liver cirrhosis by regulating Fstl1/Wnt/β-Catenin signaling pathway

Hanjing Zhangdi [a,b], Xinyu Geng [a], Ning Li [a], Ruiling Xu [a], Ying Hu [a], Jingyang Liu [a], Xu Zhang [a], Jihan Qi [a], Yingying Tian [a], Jiawei Qiu [a], Shiling Huang [a], Xueyu Cang [a], Shizhu Jin [a,*]

[a] Department of Gastroenterology and Hepatology, The Second Affiliated Hospital, Harbin Medical University, Harbin, China
[b] Future Medical Laboratory, The Second Affiliated Hospital of Harbin Medical University, Harbin, Heilongjiang, China

ARTICLE INFO

Keywords:
BMSCs
Liver cirrhosis
Fstl1
Wnt/β-Catenin

ABSTRACT

Researchers have shown that bone mesenchymal stem cells (BMSCs) can alleviate the progression of liver cirrhosis; however, it is unclear how exactly BMSCs function to cure liver disease. In this study, we used bioinformatics methods to assess differentially expressed genes (DEGs) in liver cirrhosis and found a significantly upregulated gene, Fstl1, in liver cirrhosis. In vivo and in vitro experiments showed that compared with those in the disease model group, the mRNA, and protein expression levels of Fstl1 were significantly reduced after BMSCs treatment, and the β-Catenin protein level was also significantly reduced after BMSCs treatment. Subsequently, we downregulated Fstl1 in activated hepatic stellate cells (HSCs) and found that Wnt and β-Catenin protein expression levels also decreased. Finally, we found that in BMSCs-treated activated HSCs, overexpression of Fstl1 reversed the inhibitory effect of BMSCs on the Wnt/β-Catenin signaling pathway to a certain extent. In summary, our results show that BMSCs can inhibit Wnt/β-Catenin signaling pathway activation by downregulating the protein expression level of Fstl1, thus alleviating cirrhosis. Therefore, targeted regulation of Fstl1 may provide a new therapeutic strategy for the progression of liver cirrhosis.

1. Introduction

Cirrhosis is a chronic liver disease that represents the advanced stage of several liver diseases. In recent years, its morbidity and mortality have gradually increased [1]. Cirrhosis is the 11th leading cause of mortality worldwide and claims the lives of approximately 1 million individuals annually [2]. In 2017, 1.32 million patients died of cirrhosis worldwide, accounting for 2.4 % of all-cause deaths worldwide [3]. The main factors of cirrhosis include hepatitis B virus infection, alcohol consumption, hepatitis C virus infection, nonalcoholic fatty liver disease, and autoimmune liver disease [4], which are characterized by chronic necrotizing inflammation and fibrosis. Cirrhosis and its complica tions may progress to hepatocellular carcinoma[5]. At present, medical treatment for decompensated cirrhosis is not effective, and orthotopic liver transplantation is the only effective treatment. However, due to high medical costs, a shortage of donor liver sources, many postoperative complications, lifelong immune rejection, and other factors, the wide application of orthotopic liver transplantation in clinical practice is greatly limited. At present, it is important to explore effective

* Corresponding author.
E-mail address: drshizhujin@hrbmu.edu.cn (S. Jin).

https://doi.org/10.1016/j.heliyon.2023.e21010
Received 14 May 2023; Received in revised form 30 September 2023; Accepted 12 October 2023
Available online 20 October 2023

treatment methods to block the progression of cirrhosis or reduce the degree of cirrhosis[6–8].

Hepatic stellate cells (HSCs) serve a crucial role in the pathogenesis of cirrhosis. In the normal liver, quiescent HSCs account for approximately 15 % of all resident liver cells. HSCs are located between sinusoidal endothelial cells and hepatocytes and are in the subendothelial space of Disse. The physiological function of quiescent HSCs in the liver is mainly vitamin A metabolism and fat storage. In response to pathogenic factors, HSCs differentiate from lipid-storing pericytes into myofibroblasts, resulting in a large amount of type I collagen production, which causes extracellular matrix deposition and forms cirrhotic pseudo lobules [9]. In addition, the TGF-β1/smad3 [10] and Wnt/β-Catenin signaling pathways [11] can enhance HSCs activation and promote cirrhosis.

As pluripotent stem cells, mesenchymal stem cells can differentiate into a variety of tissue cells and have received extensive attention in a variety of refractory diseases [12]. Many basic and clinical studies have shown that mesenchymal stem cells have good therapeutic effects on liver cirrhosis [13]. Mesenchymal stem cells (MSCs) have many advantages, such as wide availability, weak surface antigenicity, weak immunogenicity, attraction to damage sites and of the ability to protect normal tissue [14]. Previous studies have shown that MSCs secrete cytokines that can directly act on activated HSCs and inhibit HSCs activation and α-SMA expression. Parekkadan [15] found that BMSCs-derived interleukin-10 and tumor necrosis factor-α (TNF-α) could inhibit HSCs proliferation and collagen synthesis in cocultures of BMSCs and HSCs. Feng [16] believes that BMSCs treatment inhibits liver fibrosis by down-regulating the lnc-BIHAA1/rno-miR-667–5p signaling pathway in HSCs. Chen's [17] study found that BMSCs alleviate liver fibrosis by regulating LMO7-AP1-TGFβ signaling pathway. The mechanism by which BMSCs are involved in the treatment of cirrhosis is still being explored. This experiment was performed to examine BMSCs-mediated inhibition of HSCs activation to study how BMSCs are involved in the treatment of liver cirrhosis.

2. Materials and methods

2.1. Extraction and culture of BMSCs

After the mice were euthanized, they were immersed in 75 % ethanol, both tibias and femurs were removed under sterile conditions, and both ends of the tibial and femoral epiphyses were removed. After the bone marrow cavity was washed with PBS, the cell suspension was blown to make the cells flow out, which was repeated 3 times. The suspension of bone marrow cells was centrifuged at 1000 r/min for 5 min, the supernatant was removed, and the cell precipitate was resuspended, which was repeated 3 times. The cell suspension was mixed with a low-glucose DMEM medium containing 10 % FBS (ScienCell, USA) and seeded in cell culture flasks. The culture environment was a sterile environment at 37 °C with 5 % CO_2. P0 generation BMSCs were passaged at 1:2 after reaching 80 % adherent growth.

2.2. Identification of BMSCs

P3 generation BMSCs were collected for flow cytometry. 1×10^5 BMSCs were incubated with antibodies against CD29 (FITC), CD90 (PE), CD31 (APC) and CD43 (PerCP) (BD Biosciences, USA) for 30 min at 4 °C in the dark and washed 3 times with PBS. The cells were detected by a FACSCanto II flow cytometer (BD Biosciences, USA).

Osteogenic and adipogenic differentiation of P3 BMSCs was induced. After 14 days of osteogenic induction (Cyagen US Inc., USA), alizarin red staining showed the formation of calcium nodules. After 14 days of adipogenic induction, lipid droplet formation was detected by oil red O staining.

2.3. Animal model establishment

The liver cirrhosis model was established in 6-week-old BALB/c male mice. The grouping was as follows: normal mice were used as the control group (Control); mice intraperitoneal injection with 20 % concentration of CCl_4 (dissolved in olive oil) for 12 weeks were used as the experimental group (CCl_4); and after 8 weeks of CCl_4 injection, BMSCs were injected into the tail vein of mice for 4 weeks for the treatment group (CCl_4 +BMSCs). Eight weeks after the injection of CCl_4, the mice were injected with PBS through the tail vein for 4 weeks as the treatment negative control group (CCl_4 +PBS). The BMSCs were labelled with DiR fluorescent dye and transplanted through the mouse tail vein.

2.4. Animal in vivo imaging

After the mice were euthanized, the fresh parenchymal organs, such as the liver, heart, spleen, lung, pancreas, and kidney, were separated and a fluorescence imaging device was used to monitor the fluorescence intensities of the organs (IVIS, Night OWL II LB983, Germany).

2.5. Cell culture and coculture

The mouse hepatic stellate cell line JS1 was purchased from Otwo Biotech (Shenzhen, China) and grown in high glucose DMEM containing 10 % FBS (Corning, USA) in a 37 °C sterile environment with 5 % CO2. JS1 cells were activated by 50 ng/ml TGF-β1 (Peprotech, USA) for 48 h.

Logarithmic-grown JS1 cells were seeded in the lower chamber of a 6-well Transwell system and cultivated in high-glucose DMEM

with 10 % FBS. BMSCs suspension was added to the upper chamber and cocultured with JS1 cells for 48 h.

2.6. Cell transfection

Fstl1-siRNA and NC (negative control) siRNA were constructed by Shanghai GenePharmaCo., Ltd. siRNA of Fstl1 sense sequence: 5′– GCAAUGACCUGUGAUGGAATT –3′, antisense sequence: 5′– UUCCAUCACAGGUCAUUGCTT –3′); NC for siRNA (sense sequence: 5′– UUCUCCGAACGUGUCACGUTT –3′, antisense sequence: 5′– ACGUGACACGUUCGGAGAATT –3′). Transfection of siRNA into JS1 cells was performed with X-treme (Roche, USA). Fstl1-pcDNA3.0 vector and pcDNA3.0 empty vector were constructed by Shanghai Genechem Co., LTD. Transfection of pcDNA into JS1 cells was performed with Lipo2000 (Invitrogen, USA).

2.7. Immunofluorescence

The JS1 cells were fixed with 4 % paraformaldehyde, permeabilized with 0.1 % Triton X-100 for 15 min, and blocked with 3 % BSA for 30 min. Anti-Fstl1 primary antibody (1:100) was added to the cell slides and incubated overnight at 4 °C. After washing with PBS, the secondary antibody with an excitation wavelength of 594 nm was added dropwise and incubated in the dark for 4 h at 4 °C. After washing with PBS, the anti-β-Catenin primary antibody (1: 50) was added and incubated overnight at 4 °C environment. After washing with PBS, the secondary antibody with an excitation wavelength of 488 nm was added dropwise and incubated in the dark for 4 h at 4 °C. After washing with PBS, DAPI was added dropwise and incubated in the dark for 15 min, and then, the slides were sealed. After that, images were taken by laser scanning confocal microscopy (Carl Zeiss Microscopy GmbH, Jena, Germany). The confocal cross-section fluorescence intensity was analyzed by Origin 2017 and ImageJ software.

2.8. Immunohistochemistry

Paraffin sections of the liver tissue were prepared after fixation with 4 % paraformaldehyde for 12 h. The sections were placed in an 80 °C thermostat and heated overnight at a thickness of 3 μm. After that, xylene and alcohol were used for gradient dewaxing, 3 % H_2O_2 was used to inactivate endogenous peroxidase, and ethylenediamine tetra acetic (EDTA) was used for antigen retrieval. Then, the sections were sealed with bovine serum albumin (BSA) to block nonspecific binding, and a primary antibody was added and incubated with the sections at 4 °C overnight. The primary antibodies used were anti-Fstl1 antibody (1:400, Abcam), anti-α-SMA antibody (1:500, Abcam), and anti-β-Catenin antibody (1:300, Abcam). On the second day, the sections were incubated with goat anti-rabbit secondary antibody (Proteintech ， USA) at 37 °C for 1 h without light. The sections were washed again with PBS, and the chromogenic substrate diaminobenzidine (DAB) (Zhongshan Golden Bridge Biotechnology, Beijing, China) was dropped on the sections. Staining was terminated when the positive cells were deeply stained but the background was unstained or lightly stained, as determined by viewing under a microscope. The sections were redyed with hematoxylin, fully rinsed with water, dehydrated with gradient alcohol and xylene, sealed with the appropriate resin, dried, and photographed under an optical microscope (Nikon Corp. Tokyo, Japan). Semiquantitative analysis was performed with Image-Pro Plus 6.0 software.

2.9. Pathological staining

The liver tissue was fixed in 4 % paraformaldehyde, embedded in paraffin, and sliced. The slice thickness was 3 μm. After xylene and gradient alcohol dewaxing, the sections were stained. H&E staining, Masson staining, and Sirius red staining were performed. After the neutral gum seal was dried, the image was taken by a microscope.

2.10. Liver function

Fresh frozen liver tissues were homogenized with PBS at 4 °C according to the manufacturer's protocol. Liver function was evaluated by measuring the levels of alanine aminotransferase (ALT) (Nanjingjiancheng, China) and aspartate aminotransferase (AST). The results were detected by a microplate reader at 510 nm wavelength.

2.11. Hydroxyproline assay

Fresh frozen liver tissues were homogenized with normal saline at 4 °C according to the manufacturer's protocol. The hydroxyproline level of the liver reflects fibrosis. The results were detected by a microplate reader at 550 nm wavelength.

2.12. Real-time quantitative PCR

Total RNA from liver samples and JS1 cells were extracted by TRIzol reagent (TaKaRa, Japan) according to the manufacturer's instructions. cDNA was produced by reverse transcription using a Transcriptor First Strand cDNA Synthesis Kit (TaKaRa, Japan). The template DNA was amplified by real-time quantitative PCR (qPCR) using the Fast Start Universal SYBR Green Master kit (TaKaRa, Japan). The relative gene expression levels were normalized to GAPDH using the 2-ΔΔCT quantitation method. The q-PCR primers are shown below: Fstl1 F: TAGGCGGCAGGCACATATCTAGG, R: GAGGCGGCGAGAGCATTTCAG; GAPDH F: CAAGAAGGTGGTGAAGCAGG, R: GGCCGG CCACCCTGTTGCTGTAGCC.

2.13. Western blot analysis

Proteins of JS1 cells and liver tissues were extracted on ice. After addition of RIPA lysis protein, the supernatant was collected by centrifugation. The supernatant was collected for concentration measurements and boiled for preservation or subsequent experiments. The same amount of protein from each group was added to an SDS-PAGE gel and subjected to electrophoresis. The protein in the SDS-PAGE gel was transferred to a polyvinylidene fluoride (PVDF) membrane (Millipore, USA). Then, the membrane was blocked with 5 % skim milk for 1 h at room temperature and incubated with primary antibodies (anti-Fstl1 antibody, 1:1000, Proteintech; anti-α-SMA, 1:4000, Abcam; anti-collagen 1, 1:1000, Santa Cruz Biotechnology; anti-β-Catenin, 1:1000, Abcam; anti-Wnt, 1:3000, Proteintech; anti-GAPDH antibody, 1:10000, Proteintech) at 4 °C overnight. Thereafter, the membrane was further incubated with the corresponding secondary antibody (1:10000, Proteintech) at 37 °C for 50 min. Enhanced chemiluminescence (ECL) solution was used to visualize protein bands, and the relative protein level was calculated based on the housekeeping gene content with ImageJ.

2.14. Bioinformatics analysis

We first performed RNA-seq analysis on liver samples from control and cirrhotic mice. According to the screening threshold of $p < 0.05$ and a fold change$\geq$1.5, the volcanic and heatmaps generated by the R language software package ggpubr were used to display the screened DEGs. Subsequently, for analysis of the function of DEGs in liver fibrosis, online annotation, visualization, and integrated discovery databases were used by DAVID 6.8. When p was <0.05, the enrichment difference was considered significant. The analysis results are displayed in the bubble diagram using the R language package ggplot. Finally, we highlighted the differential expression of Fstl1 in liver samples of mice with and without liver fibrosis through the R language package ggpubr and expressed it in a box diagram.

2.15. Statistics

Each experiment was repeated at least 3 times. All data are expressed as X±SEM. GraphPad Prism 9.0 (GraphPad Prism Software, San Diego, CA, USA) was used for statistical analysis. One-way analysis of variance (ANOVA) was used for the above data, and a two-tailed Student's *t*-test was used for comparisons between the two groups. $P < 0.05$ was considered statistically significant.

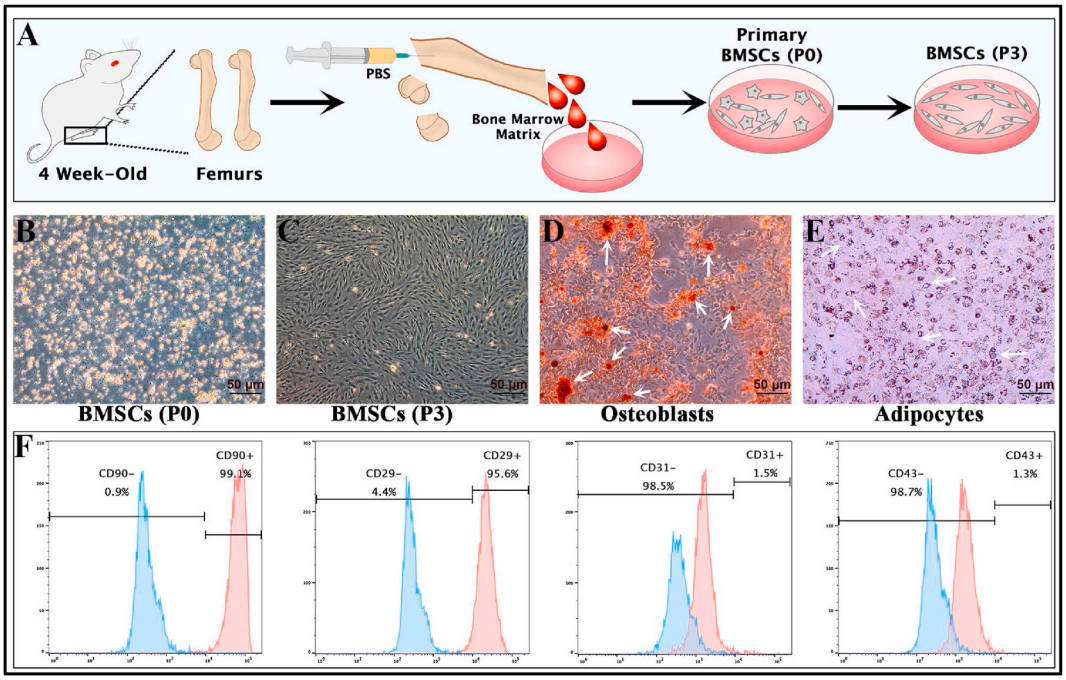

Fig. 1. Extraction and identification of mouse BMSCs. A. Schematic diagram of the extraction of mouse BMSCs.
B and C. Cell morphology of BMSCs at P0 and P3 generations.
D and E. Osteogenic and adipogenic capacity of BMSCs at P3 generation. Arrows indicate calcium nodules and lipid droplets.
F. Flow cytometry identification of BMSCs at P3 generation.
Scale bar: 50 μm.

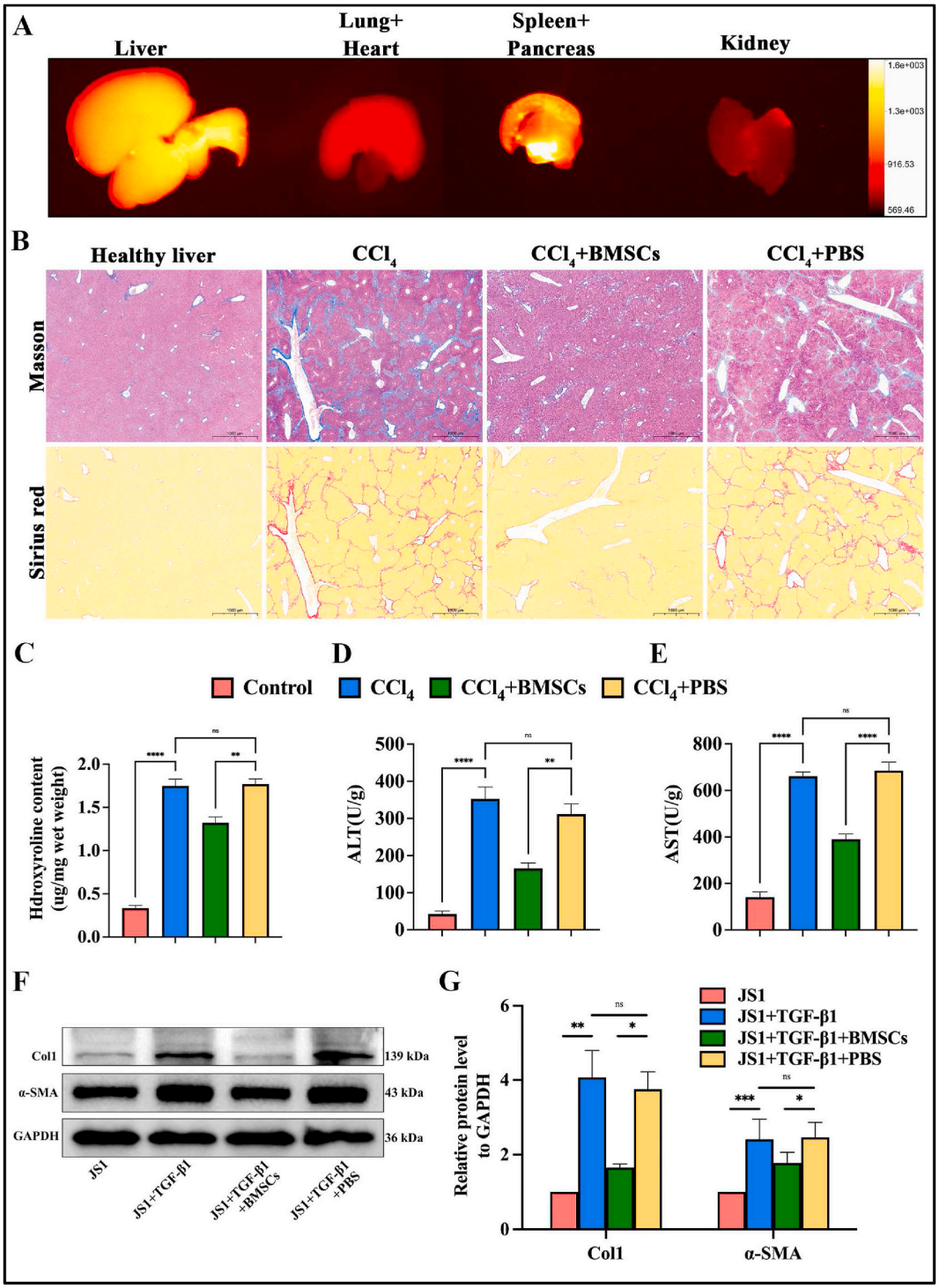

Fig. 2. BMSCs treatment alleviates the degree of cirrhosis in vitro and in vivo. A. Ex vivo organ imaging of mice after tail vein injection of BMSCs. Mouse was divided into the following 4 groups: Control, CCl_4, CCl_4 +BMSCs, CCl_4 +PBS.
B. Masson and Sirius Red staining were applied to assess the degree of cirrhosis in each group
C. Assessment of liver fibrosis level in each group by measuring hydroxyproline. D and E. Assessment of liver function in each group by measuring ALT and AST. JS1 was divided into 4 groups as follows: JS1, JS1+TGF-β1, JS1+TGF-β1+BMSCs, JS1+TGF-β1+PBS. F and G. Western Blot were applied to detect the expression levels of Col1 and α-SMA proteins in each group. Scale bar: 1000 μm ns $P \geq 0.05$, *$P < 0.05$, **$P < 0.01$, ***$P < 0.001$, ****$P < 0.0001$.

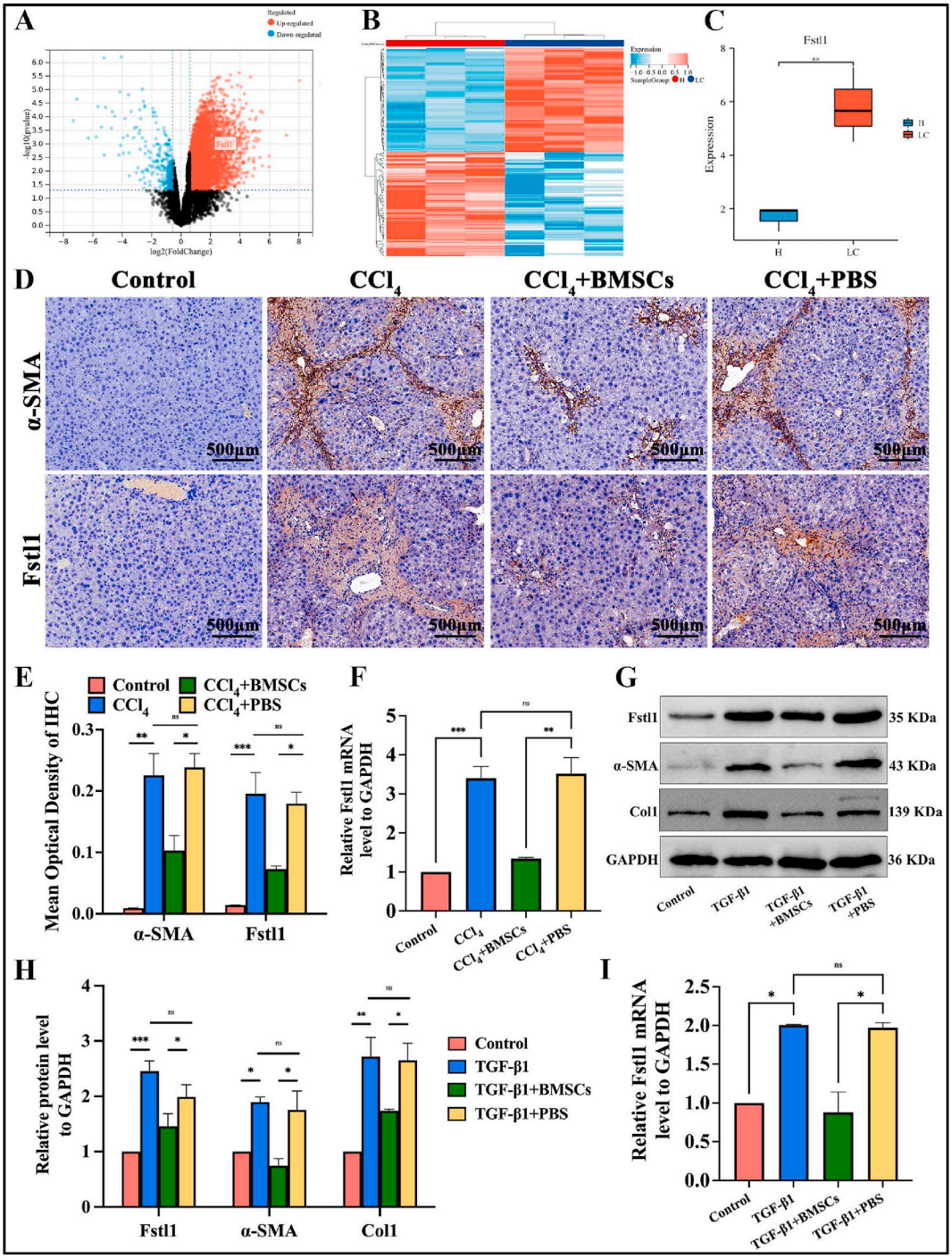

Fig. 3. BMSCs treatment down-regulates Fstl1 expression during the progression of cirrhosis both in vivo and in vitro. A and B. Volcano and heat maps of differentially expressed genes in normal and cirrhotic tissues. C. Fstl1 expression abundance in normal and cirrhotic tissues. Mouse was divided into the following 4 groups: Control, CCl_4, CCl_4 +BMSCs, CCl_4 +PBS. D and E. Immunohistochemistry were applied to detect the positivity of α-SMA and Fstl1 proteins in each group. F. qRT-PCR was applied to detect the mRNA level of Fstl1 in each group. JS1 was divided into the following 4 groups: JS1, JS1+TGF-β1, JS1+TGF-β1+ BMSCs, JS1+TGF-β1+PBS. G and H. Western Blot was applied to detect the expression levels of Fstl1, Col1 and α-SMA proteins in each group. I. qRT-PCR was applied to detect the mRNA level of Fstl1 in each group. Scale bar: 500 μm ns $P \geq 0.05$, $^{*}P < 0.05$, $^{**}P < 0.01$, $^{***}P < 0.001$.

3. Results

3.1. Extraction and identification of mouse BMSCs

BMSCs were extracted and cultured from the bilateral femurs of mice (Fig. 1A). The newly extracted P0 BMSCs were round and suspended in the cell culture medium (Fig. 1B). The cells were purified to the P3 generation after adherent passage, and the cell morphology was long and fusiform (Fig. 1C). The osteogenic (Fig. 1D) and adipogenicity (Fig. 1E) differentiation of P3 BMSCs was induced. Calcium nodule formation and fat droplet formation confirmed that BMSCs had differentiation potential. Flow cytometry results showed that stem cell surface-specific antigens CD90 and CD29 were positive, while hematopoietic stem cell surface-specific antigens CD31 and CD43 were negative (Fig. 1F). The above results confirmed the successful extraction of BMSCs.

3.2. BMSCs treatment alleviates the degree of cirrhosis in vivo and HSCs activation in vitro

DiR-labelled BMSCs were injected into the tail vein of mice, and the fluorescence intensity of each parenchymal organ was detected by a fluorescence imaging system. The results showed that the fluorescence signal was higher in the liver, spleen, and pancreas and lower in the heart, lung, and kidney. The fluorescence intensity of the liver was the highest (Fig. 2A). Subsequently, the liver of each group was stained pathologically. Masson staining and Sirius red staining showed that the livers of the CCl_4 model group had cirrhosis-related pseudo lobule formation and collagen deposition, forming a cirrhosis model. The CCl_4 model mice intraperitoneally injected with PBS also had pseudo lobule formation and collagen deposition. Compared with that in the cirrhosis group, the degree of cirrhosis in the BMSCs treatment group was decreased (Fig. 2B). Determination of hydroxyproline content in the liver was performed. The degree of liver cirrhosis was quantitatively shown. The hydroxyproline content in the BMSCs treatment group was significantly lower than that in the PBS control treatment group (Fig. 2C). The liver function of mice was evaluated by ALT and AST assays. Compared with that of the PBS control group, the liver function of the BMSCs treatment group was significantly alleviated (Fig. 2D–E). BMSCs play a therapeutic role in alleviating the progression of cirrhosis. In vitro, TGF-β1 was used to induce the activation of the mouse hepatic stellate cell line JS1. Compared with that of the activated JS1 cell control group, the surface marker protein α-SMA of activated JS1 cells and collagen 1 produced by activated cells were significantly reduced after BMSCs treatment (Fig. 2F–G).

3.3. BMSCs treatment down-regulates Fstl1 expression during the progression of cirrhosis both in vivo and in vitro

Based on the analysis of our previous experimental results [18], taking the adjusted p value less than 0.05 and the logFC value greater than 0.5 as the standard, we found a total of 2115 DEGs, of which 2225 were upregulated and 110 were downregulated. The heatmap (Fig. 3A) and volcano map (Fig. 3B) showed the distribution of overall DEGs. Subsequently, we analyzed the expression differences of Fstl1 between different samples (Fig. 3C). We found that the expression of Fstl1 was significantly upregulated in cirrhotic tissues.

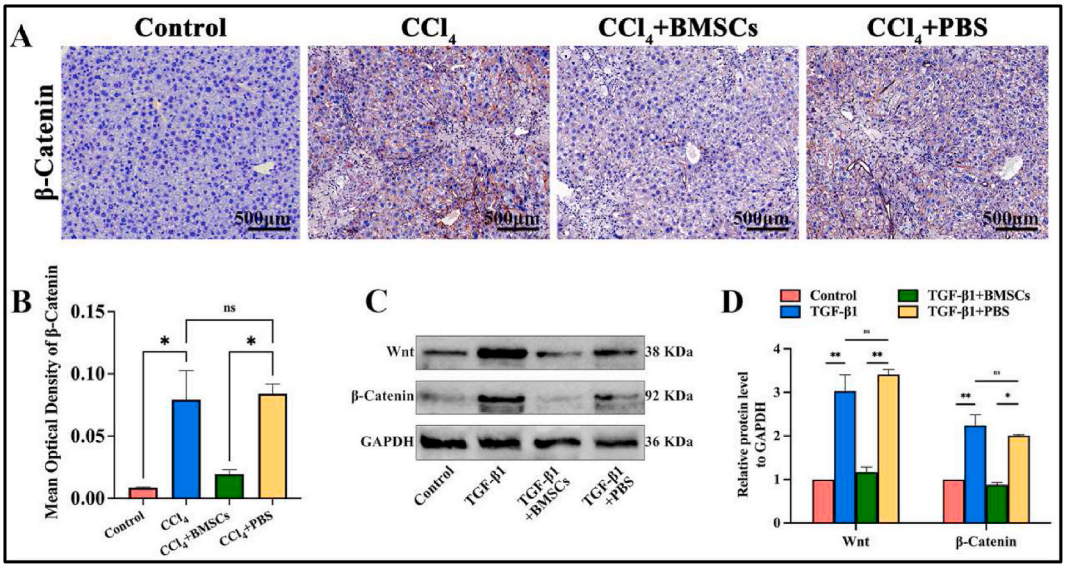

Fig. 4. BMSCs treatment inhibits the Wnt/β-Catenin signaling pathway during cirrhosis progression in vivo and in vitro. In vivo, mice were divided into 4 groups: Control, CCl_4, CCl_4 +BMSCs, CCl_4 +PBS. A and B. immunohistochemistry was applied to detect the positive rate of β-Catenin proteins in each group. In vitro, JS1 cells were divided into the following 4 groups: JS1, JS1+TGF-β1, JS1+TGF-β1 +BMSCs, JS1+TGF-β1+PBS. C and D. Western Blot was applied to detect the expression levels of Wnt and β-Catenin proteins in each group. Scale bar: 500 μm ns $P \geq 0.05$, $^*P < 0.05$, $^{**}P < 0.01$.

Mice were divided into four groups: control, CCl_4, CCl_4 +BMSCs, and CCl_4 +PBS. Through immunohistochemical analysis, we found that the protein expression of α-SMA and Fstl1 was upregulated in the livers of mice with CCl_4 -induced liver cirrhosis compared with normal livers. While both α-SMA and Fstl1 expression in the CCl_4 group was downregulated compared with that in the CCl_4 +BMSCs group, we found that BMSCs treatment can partially reverse this phenomenon (Fig. 3D and E). We also verified the mRNA expression level of Fstl1 (Fig. 3F), and the results showed that the mRNA expression level of Fstl1 was consistent with the change in its

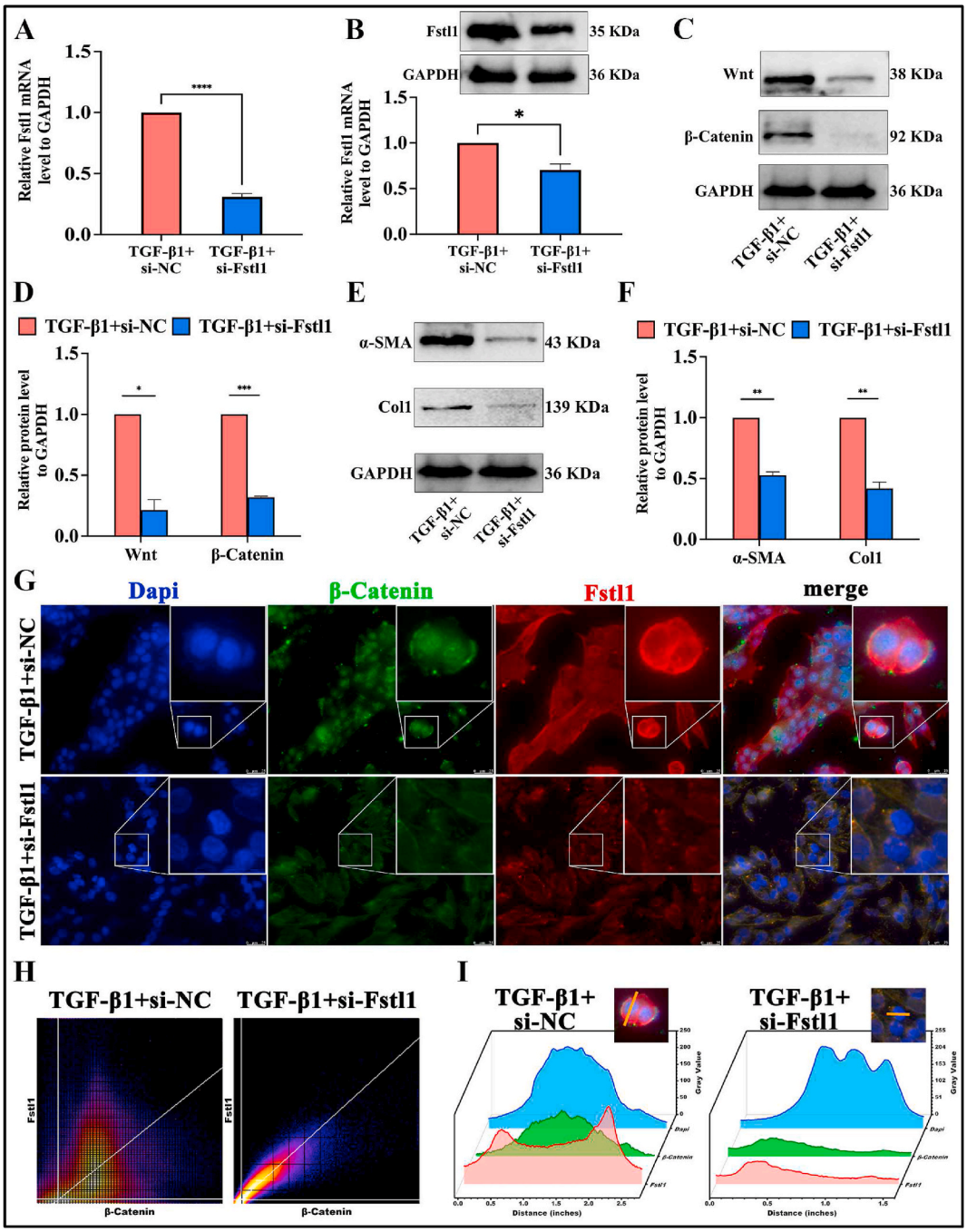

Fig. 5. Silencing of Fstl1 inhibits the activation of Wnt/β-Catenin signaling pathway. A and B. qRT-PCR and Western Blot were applied to detect the silencing efficiency of Fstl1 in activated JS1. C and D. Western Blot was applied to detect the protein expression levels of Wnt and β-Catenin after silencing of Fstl1 in activated JS1. E and F. Western Blot was applied to detect the protein expression levels of Col1 and α-SMA after silencing Fstl1 in activated JS1. G. Immunofluorescence of Fstl1 and β-Catenin in activated JS1. H. Scatter plots of Fstl1 and β-Catenin levels. I. Cross section fluorescence intensity analysis of the colocalization sites. Scale bar: 25 μm*$P < 0.05$, **$P < 0.01$, ***$P < 0.001$, ****$P < 0.0001$.

protein expression level. Subsequently, we verified the protein expression levels and the mRNA expression level in vitro. The Western blot results showed that compared with that of the control group, after TGF-β1 treatment, the expression of α-SMA and Fstl1 was upregulated. After BMSCs treatment, the expression of α-SMA and Fstl1 was downregulated (Fig. 3G and H). In addition, the expression of Fstl1 was consistent with the change in its protein expression level (Fig. 3I).

3.4. BMSCs treatment inhibits the Wnt/β-Catenin signaling pathway during cirrhosis progression in vivo and in vitro

To explore the downstream mechanism of BMSCs in alleviating liver cirrhosis, we divided mice into the following four groups: control, CCl_4, CCl_4 +BMSCs, and CCl_4 +PBS. Through immunohistochemical analysis, we found that the protein expression of β-Catenin was upregulated in CCl_4 -induced cirrhotic mice compared with control mice, while after BMSCs treatment, β-Catenin expression decreased (Fig. 4A and B). We believe that BMSCs treatment could partially reverse this phenomenon. This result was also verified in vitro experiments. Through Western blot experiments, we found that the protein expression of β-Catenin and Wnt was upregulated in TGF-β1-activated JS1 cells compared with the controls, and BMSCs treatment partially reversed this phenomenon (Fig. 4C and D). This finding suggests that BMSCs may alleviate the degree of cirrhosis through the Wnt/β-Catenin signaling pathway.

3.5. Silencing of Fstl1 inhibits the activation of Wnt/β-Catenin signaling pathway

To clarify the regulatory relationship between Fstl1 and the Wnt/β-Catenin signaling pathway in cirrhosis, we first transfected si-NC and si-Fstl1 into activated JS1 cells, and qRT−PCR (Fig. 5A) and Western blotting (Fig. 5B) verified the silencing efficiency of Fstl1. Subsequently, Western blot analysis showed that si-Fstl1 activated JS1 cells and downregulated the protein expression of the Wnt/β-Catenin pathway (Fig. 5C and D). We believe that silencing Fstl1 can reduce the protein expression levels of Wnt/β-Catenin. Moreover, silencing Fstl1 reduced the protein expression levels of α-SMA and Col1 (Fig. 5E and F). We also verified this conclusion by immunofluorescence experiments. si-Fstl1 promoted the transfer of β-Catenin from the nucleus to the cytoplasm and inhibited the Wnt/β-Catenin signaling pathway (Fig. 5G–I). This finding indicates that Fstl1 can regulate the Wnt/β-Catenin signaling pathway in TGF-β1-activated JS1 cells.

3.6. BMSCs treatment alleviates cirrhosis through Fstl1 inhibition of Wnt/β-Catenin signaling pathway

We further verified the relationship between Fstl1 and the Wnt/β-Catenin signaling pathway in the mechanism underlying BMSCs-mediated treatment of cirrhosis. We divided JS1 cells into the following four groups: TGF-β1, TGF-β1+BMSCs, TGF-β1+BMSCs + OE-

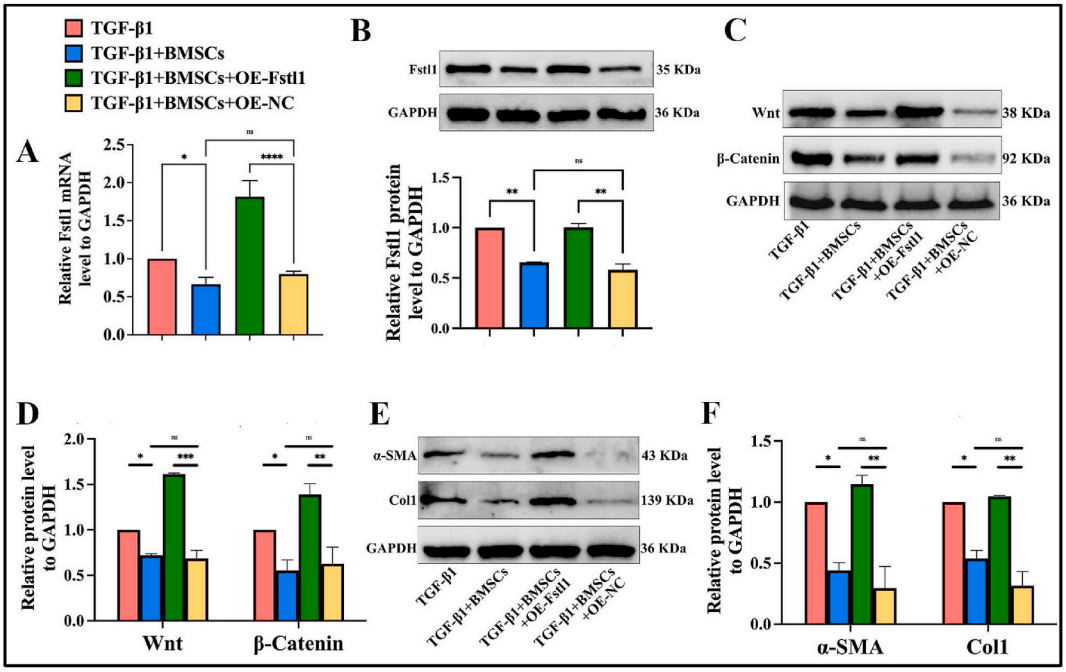

Fig. 6. BMSCs treatment alleviates cirrhosis through Fstl1 inhibition of Wnt/β-Catenin signaling pathway. JS1 was divided into the following 4 groups: JS1, JS1+TGF-β1, JS1+TGF-β1+ BMSCs, JS1+TGF-β1+PBS. A. qRT-PCR was applied to detect the mRNA expression levels of Fstl1 in each group. B. Western Blot was applied to detect the protein expression level of Fstl1 in each group. C and D. Western Blot was applied to detect the expression levels of Wnt and β-Catenin proteins in each group. E and F. Western Blot was applied to detect the expression level of Col1 and α-SMA protein in each group. ns $P \geq 0.05$, *$P < 0.05$, **$P < 0.01$, ***$P < 0.001$.

Fstl1, and TGF-β1+BMSCs + OE-NC. First, we transfected OE-NC and OE-Fstl1 into JS1 cells and used qRT−PCR (Fig. 6A) and Western blotting (Fig. 6B) to verify the overexpression efficiency of Fstl1. Subsequently, Western blot analysis showed that overexpression of Fstl1 in activated JS1 cells reversed the inhibitory effect of BMSCs treatment on the expression levels of the β-Catenin and Wnt proteins (Fig. 6C and D). We also found that overexpression of Fstl1 could reverse the inhibitory effect of BMSCs treatment on the expression levels of the α-SMA and Col1 proteins (Fig. 6E and F). These data indicate that BMSCs can alleviate cirrhosis through the Fstl1-Wnt/β-Catenin signaling pathway.

4. Discussion

Liver cirrhosis is a chronic disease. Many liver diseases progress to cirrhosis without timely and effective treatment [19]. At present, there is still no clear method to cure liver cirrhosis. Recent studies have reported that stem cell therapy can alleviate the progression of cirrhosis [20]. In this study, we explored the molecular mechanism of bone marrow mesenchymal stem cells in the treatment of liver cirrhosis (Fig. 7).

Previous studies have found that pluripotent stem cells, such as bone marrow mesenchymal stem cells [21,22], adipose mesenchymal stem cells [23], and hair follicle stem [24], can alleviate the progression of cirrhosis. In this study, we selected the most accessible and effective cells, BMSCs, for the treatment of liver cirrhosis and studied their mechanism. In vivo experiments showed that transplanted BMSCs were recruited to the inflamed liver by DiR fluorescence labelling of BMSCs. By comparing liver function and hydroxyproline expression in the livers of mice in the cirrhosis group and the BMSCs treatment group, we found that BMSCs could alleviate the progression of cirrhosis and thus play a therapeutic role. In vitro experiments, we selected the important hepatic stellate cells that lead to the appearance of pseudo lobules in cirrhosis [25]. TGF-β1induced activation of the mouse hepatic stellate cell line JS1 [10]. By comparing the activated JS1 cells with the activated JS1 cells after BMSCs treatment, we found that the production of collagen 1 protein decreased, and the surface marker α-SMA protein representing the activation of JS1 cells decreased. BMSCs reduce collagen production by inhibiting the activation of hepatic stellate cells, thereby alleviating cirrhosis in vivo.

In this study, we analyzed the sequencing results of cirrhotic mice [18] and found that the expression of Fstl1 was increased in cirrhotic mice compared with healthy mice, which was consistent with the report that Fstl1 played a role in fibrotic diseases. Experimental studies have confirmed that the expression of Fstl1 is increased in myocardial infarction [26], pulmonary fibrosis [27], chronic nephritis renal fibrosis [28] and liver fibrosis [29]. Since cirrhosis is the end stage of liver fibrosis, the increase of Fstl1 in cirrhosis tissues in this study has research value. In addition, we verified that after BMSCs treatment in mice and in vitro, the expression of Fstl1 was lower than that in the disease group, which indicated that BMSCs treatment of liver cirrhosis was achieved by reducing Fstl1. To this end, we verified this hypothesis in vitro in JS1 cells. While BMSCs activated JS1 cells, overexpression of Fstl1 increased the activation of JS1 cells, which partially reversed the therapeutic effect of BMSCs, confirming our hypothesis that BMSCs alleviated hepatic stellate cell activation and cirrhotic progression by reducing Fstl1 expression.

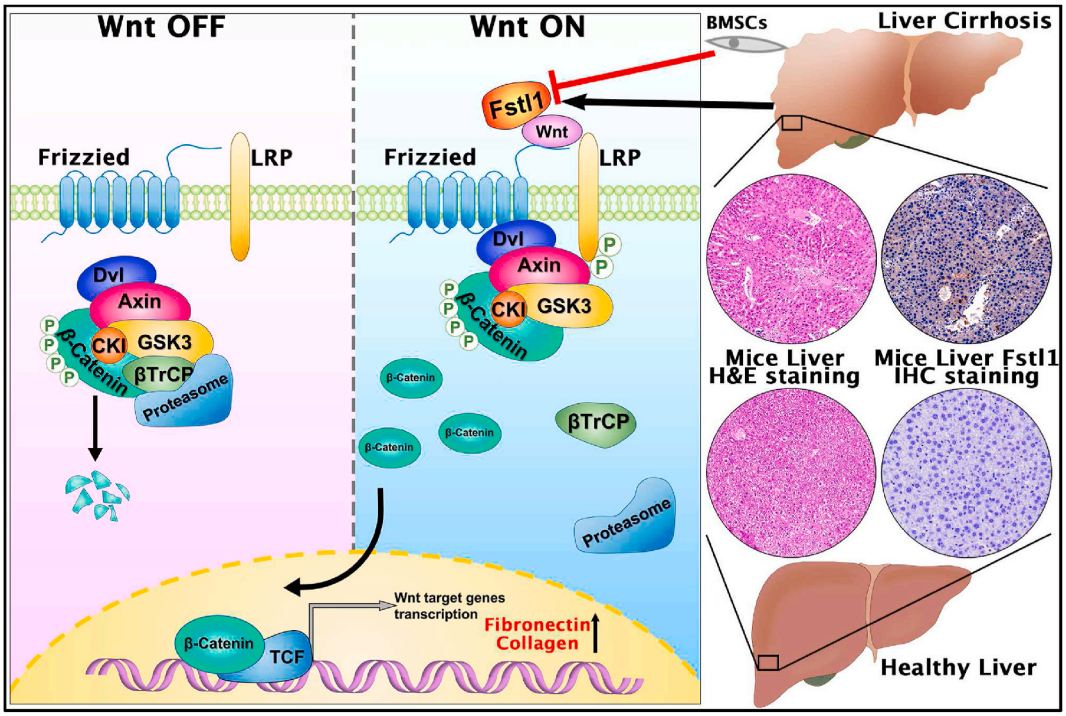

Fig. 7. Schematic representation of the mechanism of BMSCs in the treatment of cirrhosis.

Many studies have shown that the Wnt/β-Catenin pathway is involved in the development of fibrosis [30] and the occurrence of hepatocellular carcinoma [31,32]. When the Wnt/β-Catenin signaling pathway is activated, β-Catenin in the cytoplasm is dephosphorylated and translocated to the nucleus and binds to T cell factor (TCF)/Lymphoid enhancer-binding factor (LEF) to stimulate Wnt transcriptional target genes, including the expression of fibrosis-related genes, such as fibronectin and Matrix Metallo Proteinases-7 (MMP-7), to promote fibrosis. As the end stage of liver fibrosis, cirrhosis is also involved in the Wnt/β-Catenin pathway. It has been reported that rat BMSCs alleviate liver fibrosis by inhibiting the Wnt/β-Catenin pathway [33]. In this study, we used allogeneic mouse BMSCs to treat liver cirrhosis in mice and verified the downregulation of Wnt/β-Catenin protein expression after BMSCs treatment in vivo and in vitro, thus confirming that BMSCs can alleviate the progression of liver cirrhosis through the Wnt/β-Catenin pathway.

Our experiments confirmed that BMSCs can alleviate liver cirrhosis by downregulating Fstl1 expression, so we hypothesized that there is an interaction between Fstl1 and the Wnt/β-Catenin pathway. It has been confirmed that in renal fibrosis in chronic kidney disease, Fstl1 increases renal fibrosis and activates the Wnt/β-Catenin signaling pathway, while downregulation of Fstl1 inhibits the Wnt/β-Catenin signaling pathway; thus, Fstl1 is considered a new extracellular enhancer of the Wnt/β-Catenin pathway [34]. Therefore, in liver cirrhosis, we detected the protein expression of Wnt/β-Catenin by downregulating Fstl1 in JS1 cells in vitro. After downregulation of Fstl1, the protein expression of the Wnt/β-Catenin pathway decreased. Moreover, in activated JS1 cells after Fstl1 downregulation, nuclear β-Catenin expression decreased, and nuclear translocation occurred, indicating that the Wnt/β-Catenin pathway was inhibited after the downregulation of Fstl1. After verifying that Fstl1 regulates the Wnt/β-Catenin pathway, our study further confirmed the relationship between BMSCs and Fstl1 and Wnt/β-Catenin. In activated JS1 cells, the Wnt/β-Catenin pathway was inhibited after BMSCs treatment. However, overexpression of Fstl1 during BMSCs treatment alleviated the inhibition of the Wnt/β-Catenin pathway to a certain extent, thus partially reversing the therapeutic effect of BMSCs on activated JS1 cells.

Although we lack high-throughput screening procedures to support the scientific hypothesis underpinning the Fstl1/Wnt/β-Catenin pathway, we experimentally verified the reasonability of this hypothesis in liver cirrhosis. Potentially, the therapeutic effectiveness of BMSCs transplantation in clinical practice to treatment liver cirrhosis could be strengthened by adjustment of Fstl1/Wnt/β-Catenin pathway, which could promote transplanted BMSCs *trans*-differentiation to hepatocyte. Since there are risk factors for the development of HCC in liver cirrhosis, the role of Fstl1/Wnt/β-Catenin pathway in clinical liver cirrhosis needs to be further studied.

5. Conclusions

Overall, in this study, we demonstrated that BMSCs alleviated HSCs activation and liver cirrhosis by downregulating Fstl1, and Fstl1 could affect on Wnt/β-Catenin pathway. This study provides experimental data and theoretical support for further exploring the therapeutic mechanism of BMSCs in clinical application.

Ethics approval and consent to participate

All the animal experiments were performed as per the guidelines of the Experimental Center of the Second Affiliated Hospital of Harbin Medical University (Ethics Project Number: No. SYDW2021–001).

Consent for publication

Not applicable.

Data availability statement

Data will be made available on request.

Funding

This work was supported by outstanding younger funding of the Second Affiliated Hospital of Harbin Medical University (No.3 batch).

CRediT authorship contribution statement

Hanjing Zhangdi: Conceptualization, Data curation, Formal analysis, Methodology, Writing – original draft, Writing – review & editing. **Xinyu Geng:** Methodology. **Ning Li:** Methodology. **Ruiling Xu:** Methodology. **Ying Hu:** Methodology. **Jingyang Liu:** Formal analysis. **Xu Zhang:** Formal analysis. **Jihan Qi:** Formal analysis. **Yingying Tian:** Formal analysis. **Jiawei Qiu:** Formal analysis. **Shiling Huang:** Formal analysis. **Xueyu Cang:** Formal analysis. **Shizhu Jin:** Conceptualization, Investigation, Project administration, Supervision, Writing – review & editing.

Declaration of competing interest

All the authors declare that we have no competing interests.This work was supported by outstanding younger funding of the Second

Affiliated Hospital of Harbin Medical University (No.3 batch). All the animal experiments were performed as per the guidelines of the Experimental Centre of the Second Affiliated Hospital of Harbin Medical University (Ethics Project Number: No. SYDW2021–001).

Acknowledgements

We thank the support of the Experimental Animal Center of the Second Affiliated Hospital of Harbin Medical University. And we thank to professor Chunying Zhang (Department of Urology, the Second Affiliated Hospital of Harbin Medical University) and Dr Zhaozheng Li (Department of Nephrology, the Second Affiliated Hospital of Harbin Medical University) for help.

Abbreviations

α-SMA	Alpha-Smooth Muscle Actin
ALT	Alanine aminotransferase
AST	Aspartate aminotransferase
BMSCs	Bone mesenchymal stem cells
CCl_4	Tetrachloromethane
Col-1	Collagen Type 1
DiR	1- dioctadecyl - 3,3,3,3 -tetramethylindotricarbocyaine iodide
FBS	Fetal Bovine Serum
HSCs	Hepatic Stellate Cells
Hyp	Hydroxyproline
MSCs	Mesenchymal stem cells
TGF-β1	Transforming growth factor-β1

References

[1] H. Yoshiji, K. Koike, Evidence-based clinical practice guidelines for liver cirrhosis 2020, Hepatol. Res. 51 (2021) 725–749.
[2] S.K. Asrani, H. Devarbhavi, J. Eaton, P.S. Kamath, Burden of liver diseases in the world, J. Hepatol. 70 (2019) 151–171.
[3] S.G. Sepanlou, R. Malekzadeh, The global, regional, and national burden of cirrhosis by cause in 195 countries and territories, 1990–2017: a systematic analysis for the Global Burden of Disease Study 2017, The Lancet Gastroenterology & Hepatology 5 (2020) 245–266.
[4] A. Rizzo, A.D. Ricci, A. Di Federico, G. Frega, A. Palloni, S. Tavolari, G. Brandi, Predictive biomarkers for checkpoint Inhibitor-based Immunotherapy in hepatocellular carcinoma: where do we stand? Front. Oncol. 11 (2021), 803133.
[5] B. Li, C. Zhang, Y.-T. Zhan, Nonalcoholic fatty liver disease cirrhosis: a review of its epidemiology, risk factors, clinical presentation, diagnosis, management, and prognosis, Canadian Journal of Gastroenterology and Hepatology. 2018 (2018) 1–8.
[6] A.A. Patel, A.M. Walling, J. Ricks-Oddie, F.P. May, S. Saab, N. Wenger, Palliative care and health care utilization for patients with end-stage liver disease at the end of life, Clin. Gastroenterol. Hepatol. 15 (2017) 1612–1619.e4.
[7] M. Verma, E.B. Tapper, A.G. Singal, V. Navarro, Nonhospice palliative care within the treatment of end-stage liver disease, Hepatology 71 (2020) 2149–2159.
[8] W.R. Kim, J.R. Lake, J.M. Smith, M.A. Skeans, D.P. Schladt, E.B. Edwards, A.M. Harper, J.L. Wainright, J.J. Snyder, A.K. Israni, B.L. Kasiske, OPTN/SRTR 2015 annual data report: liver, Am. J. Transplant. 17 (2017) 174–251.
[9] X. Cai, J. Wang, J. Wang, Q. Zhou, B. Yang, Q. He, Q. Weng, Intercellular crosstalk of hepatic stellate cells in liver fibrosis: new insights into therapy, Pharmacol. Res. 155 (2020), 104720.
[10] Q. Liu, C. Lv, Q. Huang, L. Zhao, X. Sun, D. Ning, J. Liu, Y. Jiang, S. Jin, ECM1 modified HF-MSCs targeting HSCs attenuate liver cirrhosis by inhibiting the TGF-β/Smad signaling pathway, Cell Death Dis. 8 (2022) 51.
[11] I.H. Lee, E. Im, H. Lee, D.Y. Sim, J.H. Lee, J.H. Jung, J.E. Park, B.S. Shim, S. Kim, Apoptotic and antihepatofibrotic effect of honokiol via activation of GSK3β and suppression of Wnt/β-Catenin pathway in hepatic stellate cells, Phytother Res. 35 (2021) 452–462.
[12] Y. Shi, Y. Wang, Q. Li, K. Liu, J. Hou, C. Shao, Y. Wang, Immunoregulatory mechanisms of mesenchymal stem and stromal cells in inflammatory diseases, Nat. Rev. Nephrol. 14 (2018) 493–507.
[13] M.P. de Miguel, I. Prieto, A. Moratilla, J. Arias, M.A. Aller, Mesenchymal stem cells for liver regeneration in liver failure: from experimental models to clinical trials, Stem Cells International. 2019 (2019) 1–12.
[14] F. Marofi, G. Vahedi, A. hasanzadeh, S. Salarinasab, P. Arzhanga, B. Khademi, M. Farshdousti Hagh, Mesenchymal stem cells as the game-changing tools in the treatment of various organs disorders: mirage or reality? J. Cell. Physiol. 234 (2019) 1268–1288.
[15] B. Parekkadan, D. van Poll, Z. Megeed, N. Kobayashi, A.W. Tilles, F. Berthiaume, M.L. Yarmush, Immunomodulation of activated hepatic stellate cells by mesenchymal stem cells, Biochem. Biophys. Res. Commun. 363 (2007) 247–252.
[16] Y. Feng, Y. Li, M. Xu, H. Meng, C. Dai, Z. Yao, N. Lin, Bone marrow mesenchymal stem cells inhibit hepatic fibrosis via the AABR07028795.2/rno-miR-667-5p axis, Stem Cell Res. Ther. 13 (2022) 375.
[17] Z. Chen, D. Chen, C. Cai, L. Jin, J. Xu, Y. Tu, X. Huang, J. Xu, M. Chen, F. Xue, X. Lan, X. Wang, Y. Ge, H. Sun, Y. Chen, BMSCs attenuate hepatic fibrosis in autoimmune hepatitis through regulation of LMO7-AP1-TGFβ signaling pathway, Eur Rev Med Pharmaco 25 (2021) 1600–1611.
[18] Y. Zhang, X. Nie, Y. Jiang, L. Wang, Z. Wan, H. Jin, R. Pu, M. Liang, H. Zhang, Q. Liu, Y. Chang, Y. Gao, N. Yang, S. Jin, Comprehensive analysis of the differentially expressed transcriptome with ceRNA networks in a mouse model of liver cirrhosis, CB (Curr. Biol.) 17 (2022) 510–520.
[19] L. Man, W.Z. Qun, Z. Lu, Z. Hao, L.D. Wu, Z.M. Geng, Burden of cirrhosis and other chronic liver diseases caused by specific etiologies in China, 1990−2016: findings from the global burden of disease study 2016, Biomed. Environ. Sci. 33 (2020) 1–10.
[20] F. Nevens, S. van der Merwe, Mesenchymal stem cell transplantation in liver diseases, Semin. Liver Dis. 42 (2022) 283–292.
[21] H. Zhangdi, Y. Jiang, Y. Gao, S. Li, R. Xu, J. Shao, J. Liu, Y. Hu, X. Zhang, X. Zhang, L. Zhao, J. Qi, X. Geng, S. Jin, From phenomenon to essence: a newly involved lncRNA Kcnq1ot1 protective mechanism of bone marrow mesenchymal stromal cells in liver cirrhosis, Adv. Sci. 10 (2023), 2206758.
[22] Y. Zhang, H. Zhangdi, X. Nie, L. Wang, Z. Wan, H. Jin, R. Pu, M. Liang, Y. Chang, Y. Gao, H. Zhang, S. Jin, Exosomes derived from BMMSCs mitigate the hepatic fibrosis via anti-pyroptosis pathway in a cirrhosis model, Cells 11 (2022) 4004.

[23] A. Seki, Y. Sakai, T. Komura, A. Nasti, K. Yoshida, M. Higashimoto, M. Honda, S. Usui, M. Takamura, T. Takamura, T. Ochiya, K. Furuichi, T. Wada, S. Kaneko, Adipose tissue-derived stem cells as a regenerative therapy for a mouse steatohepatitis-induced cirrhosis model: seki, Sakai, Et al, Hepatology 58 (2013) 1133–1142.
[24] Q. Liu, C. Lv, Y. Jiang, K. Luo, Y. Gao, J. Liu, X. Zhang, J.M. Omar, S. Jin, From hair to liver: emerging application of hair follicle mesenchymal stem cell transplantation reverses liver cirrhosis by blocking the TGF-β/Smad signaling pathway to inhibit pathological HSCs activation, PeerJ 10 (2022), e12872.
[25] A. Khanam, P.G. Saleeb, S. Kottilil, Pathophysiology and treatment options for hepatic fibrosis: can it Be completely cured? Cells 10 (2021) 1097.
[26] S. Hu, H. Liu, Z. Hu, L. Li, Y. Yang, Follistatin-like 1: a dual regulator that promotes cardiomyocyte proliferation and fibrosis, J. Cell. Physiol. 235 (2020) 5893–5902.
[27] Y. Dong, Y. Geng, L. Li, X. Li, X. Yan, Y. Fang, X. Li, S. Dong, X. Liu, X. Li, X. Yang, X. Zheng, T. Xie, J. Liang, H. Dai, X. Liu, Z. Yin, P.W. Noble, D. Jiang, W. Ning, Blocking follistatin-like 1 attenuates bleomycin-induced pulmonary fibrosis in mice, J. Exp. Med. 212 (2015) 235–252.
[28] N.A. Maksimowski, X. Song, E.H. Bae, H. Reich, R. John, Y. Pei, J.W. Scholey, Nephrotic syndrome study network (NEPTUNE), follistatin-like-1 (FSTL1) is a fibroblast-derived growth factor that contributes to progression of chronic kidney disease, Indian J. Manag. Sci. 22 (2021) 9513.
[29] J. Rao, H. Wang, M. Ni, Z. Wang, Z. Wang, S. Wei, M. Liu, P. Wang, J. Qiu, L. Zhang, C. Wu, H. Shen, X. Wang, F. Cheng, L. Lu, FSTL1 promotes liver fibrosis by reprogramming macrophage function through modulating the intracellular function of PKM2, Gut 71 (2022) 2539–2550.
[30] Y. Guo, L. Xiao, L. Sun, F. Liu, Wnt/β-Catenin signaling: a promising new target for fibrosis diseases, Physiol. Res. 61 (2012) 337–346.
[31] A. Di Federico, A. Rizzo, R. Carloni, A. De Giglio, R. Bruno, D. Ricci, G. Brandi, Atezolizumab-bevacizumab plus Y-90 TARE for the treatment of hepatocellular carcinoma: preclinical rationale and ongoing clinical trials, Expet Opin. Invest. Drugs 31 (2022) 361–369.
[32] A. Rizzo, A. Cusmai, G. Gadaleta-Caldarola, G. Palmiotti, Which role for predictors of response to immune checkpoint inhibitors in hepatocellular carcinoma? Expet Rev. Gastroenterol. Hepatol. 16 (2022) 333–339.
[33] Z. Liu, S. Zhou, Y. Zhang, M. Zhao, Rat bone marrow mesenchymal stem cells (BMSCs) inhibit liver fibrosis by activating GSK3β and inhibiting the Wnt3a/β-Catenin pathway, Infect. Agents Cancer 17 (2022) 17.
[34] Y. Zhang, Y. Wang, G. Zheng, Y. Liu, J. Li, H. Huang, C. Xu, Y. Zeng, X. Zhang, J. Qin, C. Dai, H.O. Hambrock, U. Hartmann, B. Feng, K.K. Mak, Y. Liu, H.-Y. Lan, Y. Huang, Z.-H. Zheng, Y. Xia, Follistatin-like 1 (FSTL1) interacts with Wnt ligands and Frizzled receptors to enhance Wnt/β-Catenin signaling in obstructed kidneys in vivo, J. Biol. Chem. 298 (2022), 102010.